Flexural expression of European continental lithosphere under the western outer Carpathians.

Zoetemeijer, B.P.; Tomek, C.; Cloetingh, S.A.P.L.

published in
Tectonics
1999

DOI (link to publisher)
10.1029/1998TC900034

TECTONICS, VOL. 18, NO. 5, PAGES 843-861, OCTOBER 1999

Flexural expression of European continental lithosphere under the western outer Carpathians

Reini Zoetemeijer
Institute of Earth Sciences, Vrije Universiteit, Amsterdam

Čestmir Tomek
Intitut für Geologie und Paläontologie, Universität Salzburg, Salzburg, Austria

Sierd Cloetingh
Institute of Earth Sciences, Vrije Universiteit, Amsterdam

Abstract. We present the results of an analysis of the flexural down bending of the European lithosphere under the western outer Carpathians for a grid of five profiles with a lateral spacing of about 100 km crossing the Carpathians and its foreland. Seismic sections, including two deep seismic reflection lines, and numerous wells allowed us to quantify the flexural curvature of the lithosphere. In addition, gravity data are used to obtain independent constraints. Two evolutionary scenarios involving subduction/underthrusting of passive margin and a phase change in the lower crust are investigated in a context of relatively flat Moho under the area. Furthermore, recent uplift, expressing itself in erosional features observed along the distal margin of the foredeep, is quantified. The generally modest Bouguer gravity anomaly points to nonisostatic processes causing this uplift. Steeply dipping basement under the Carpathians to about 10 km depth at the location of the Pieniny Klippen Belt is explained by relatively weak lithosphere, which is expressed in the predicted low values of effective elastic thickness of 16 km decreasing locally to 3 km. The low strength of the European lithosphere in this region is probably caused by mechanical weakening controlled by partial yielding due to high flexural curvature. The weakest parts of the lithosphere along the profiles, corresponding to low effective elastic thicknesses, are concentrated in the areas of maximum bending. Predicted flexural bending stresses as a function of bending moment and effective elastic thickness increase dramatically under the outer zone of the Carpathian belt, explaining reactivations of older basement structures in these regions.

1. Introduction

Deep seismic reflection profiles through the Outer western Carpathians (e.g., the 2T line and 8HR line of *Tomek and Hall* [1993]) confirm the hypothesis of Neogene subduction/underthrusting of European lithosphere under the Carpathians [e.g. *Dewey and Bird*, 1970; *Uhlig*, 1907]. The 8HR line, parallel to profile I in Figure 1a and crossing the most southwestern part of the Carpathians, specially provides a clear image of the current plate configuration (Figure 1b). It shows a steep SE dipping (45°) European plate, which can be traced downdip to ~9 s (25-27 km) under the Carpathian mountain belt [*Tomek and Hall*, 1993].

In this paper we analyze the shape of the downbent European lithosphere under the Carpathians on the basis of detailed flexural and integrated Bouguer gravity analyses. In earlier flexural analyses [*Royden*, 1988] the Carpathian system is compared with the Adriatic system, where mainly subsurface loads control the subsidence since the generally modest topographic elevation (1000 m above sea level) cannot produce loads sufficient to explain the steep basin. The Adriatic setting, however, is also characterized by a deep negative low in the Bouguer gravity anomaly (of the order of −100 mGals or less) [e.g., *Moretti and Royden*, 1988], whereas the gravity anomaly in the western Carpathians does not show such a distinct minimum.

Judging from the variations in basin width along the western Carpathian Arc, flexural behavior of the European lithosphere is not uniform (Figure 1). In section 5 we analyze, in addition to profile 1, four seismic lines crossing the western Carpathians (Figure 1) to investigate the lateral variations in mechanical behavior of the lithosphere. These lateral variations can be caused by variations in the rheology of the downbent European lithosphere under the West Carpathians [*Lankreijer et al.*, 1999]. Alternatively, they can result from variations in the deformation mechanism(s). In the following, different hypotheses are presented in which we identify processes other than flexural processes, modifying the flexural expression under the West Carpathians. These processes are partly coeval, predating and postdating the Neogene subduction/underthrusting process.

We demonstrate that, in addition to the classification of different belts by the role of plate boundary processes and shape of the foreland basins [e.g., *Royden*, 1993], flexural modeling can be very useful in a regional study of the Carpathians in reconstructing vertical movements evaluating tectonic configurations, and verifying new hypotheses. Questions addressed in this paper are as follows: What is the process, in addition to topographic loading, that can explain the steep downbending of the European lithosphere, which results

Paper number 1998TC900034.
0278-7407/99/1998TC900034$12.00

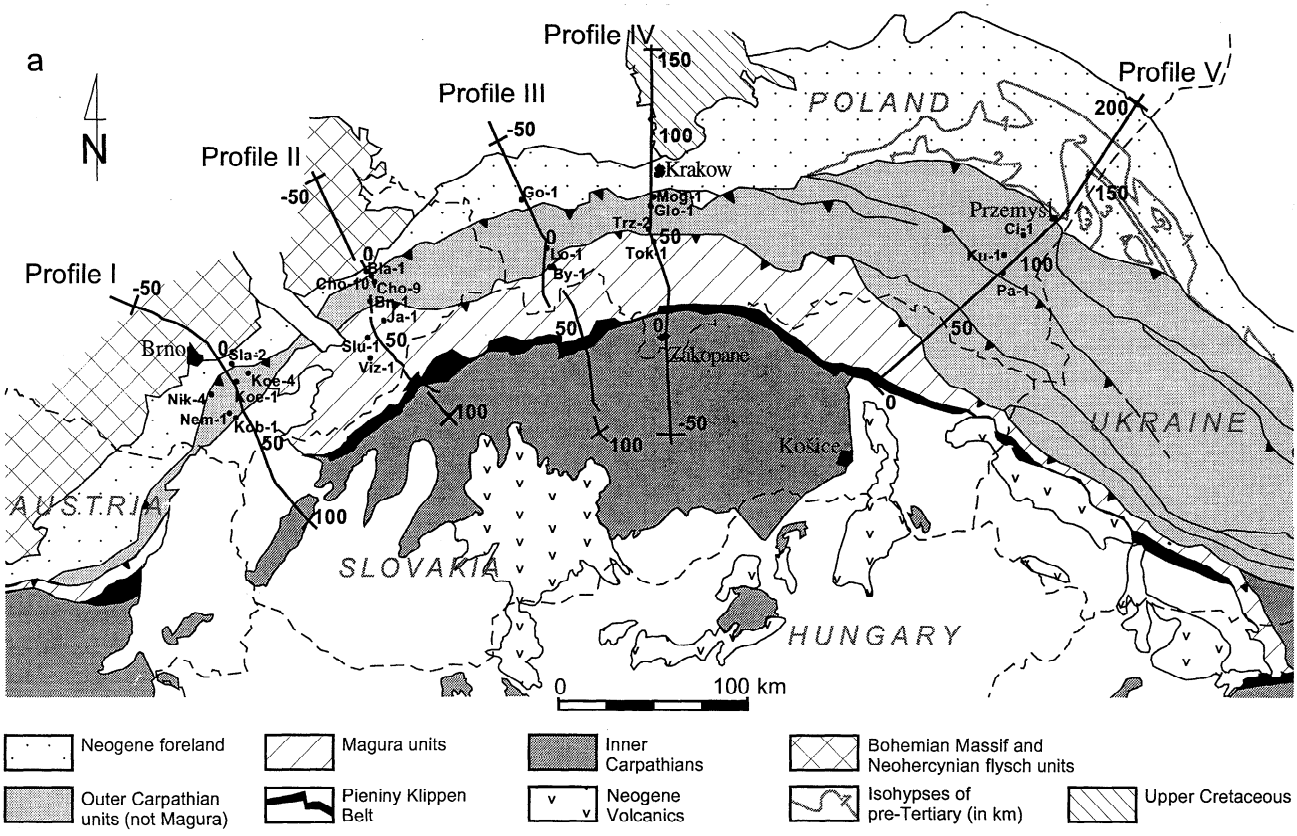

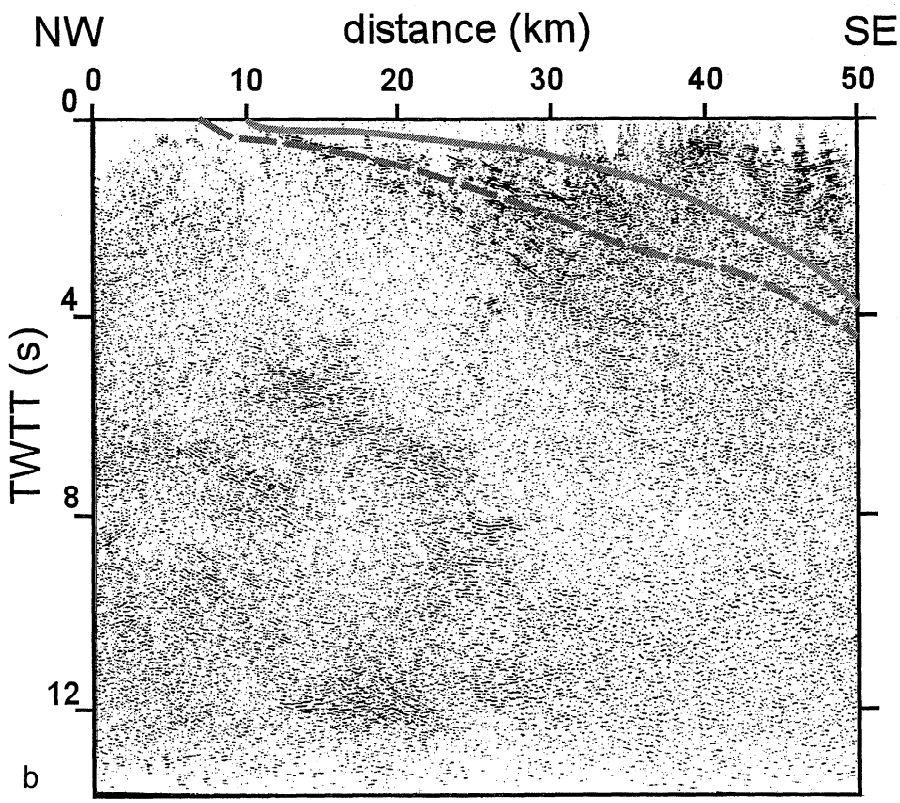

Figure 1. (a) Simplified geologic map of the western Carpathians and the position of the profiles. (b) Time deep seismic section of profile I. Solid shaded line in the base of Neogene thrust wedge; dashed shaded line is the base of Palcozoic sediments (8HR line, modified after *Tomek and Hall* [1993]). See Figure 1a for location.

in a regional isostatic equilibrium, taking into consideration the flat Moho? Does the simulated density distribution predict a gravity field that is in agreement with the observed Bouguer gravity anomaly? If not, what are the processes possibly controlling the gravity signal in the western Carpathians? In what sense is the basin geometry related to lateral changes in plate configuration? Finally, to what extend can the lithosphere support the flexural bending and does it not lose its strength? In other words, is it still possible to apply thin-elastic-plate models to these areas of highly deformed continental lithosphere?

2. Tectonic Setting

The Carpathians are an arc shaped mountain belt, which is located between the Alps in the west and the Balkans in the southeast. They are surrounded by a foredeep filled with Neogene to Quaternary clastic deposits. The Carpathians are subdivided in the western, eastern, and southern Carpathians. Here we focus on the western Carpathians and the transition area between western and eastern Carpathians. The transition between western Carpathians and eastern Carpathians is located east of the Inner West Carpathians and is covered by the East Slovakian Neogene basin, near Košice (Figure 1a). The western Carpathians are interpreted as the oldest part of the Carpathians. Subduction ceased at Karpatian time (16.8 Ma) in the west and at Late Badenian time (14-15 Ma) east of Krakow [*Oszczypko and Slaczka*, 1985]. Younger uplift, however, is recorded in the Inner Carpathians in the Tatra Mountains south of Zakopane (Figure 1a). The current topographic maximum (2655 m) of the generally modest topography of the western Carpathians is located there.

In the western Carpathians the autochthonous foredeep sediments range from Eggenburgian (~ 19 Ma) to Badenian in age [*Kovac et al.*, 1992]. In addition to the foredeep the Miocene molasse deposits are also incorporated in the folded accretionary wedge of the Outer Carpathians [*Oszczypko and Slaczka*, 1989]. Furthermore, the margin of the overriding plate is composed of two sets of older accretionary complexes: (1) Central West Carpathian nappes, emplaced in the Late Cretaceous, and (2) the Magura flysch and Pieniny Klippen, emplaced in the Paleogene [*Andrusov*, 1968; *Tomek and Hall*, 1993]. A post Middle Miocene transpressive-transtensive regime further controlled the deformation in the western Carpathians and is probably related to the formation of the Vienna basin [*Lankreijer et al.*, 1995]. The description of the complex deformation history and balancing of horizontal movements is, however, beyond the scope of this paper as we concentrate primarily on the vertical movements.

The foredeep sediments and the most distal tectonic units in the SW (Zdanice) consist of course-grained hardly consolidated sandy mica-ridge marls with low densities (2300–2400 kg/m3). In the SW this material forms a 4-km-thick thrust wedge. Along strike, more to the NE, the equivalent (Sub)Silesian units become less important relative to the Magura flysch units, consisting of sandstones and conglomerates with much larger density (2600–2700 kg/m3). Imbricate Magura nappes reach a thickness of at least 10 km close to the Pieniny Klippen Belt. In contrast to the unconsolidated marls the deposition of the Magura flysch is probably not solely related to the development of the second accretionary complex. Upper Cretaceous turbiditic deposits of the Magura unit that are now situated close to the Pieniny Klippen Belt refer to a deep marine depositional environment. *Roure et al.* [1994] argue in favor of a possible passive margin origin for the thick sedimentary sequence of the Magura.

The Pieniny Klippen Belt (PKB) is a narrow zone and reaches from near Vienna in the west to Maramures in the east. It separates the Outer Carpathians from the Inner Carpathians, forming part of the Central Carpathian domain. The contact is nearly vertical and is bounded by strike-slip faults of post-Eocene age [*Birkenmajer*, 1985]. Since the deformation in the Outer Carpathians is associated with the development of the second accretionary wedge and subduction/underthrusting of the European lithosphere, the Pieniny Klippen Belt can be treated as the backstop for this collision zone. Also, in the flexural analysis the position of the effective plate boundary in the model is in the vicinity of the PKB, except for the most eastern part in the transition area between western and eastern Carpathians, where the belt and foredeep dramatically widen. This zone forms the transition to the eastern Carpathians, where the belt changes its direction of strike to become parallel to the Tornquist Teisseyre Zone.

In the western Carpathians, volcanic activity during the Neogene is not as clearly associated to the subduction as in the eastern Carpathians, where volcanic bodies are parallel to the chain and linear in time [*Downes and Vaselli*, 1995]. However, under the Danube basin major subsurface bodies of Neogene volcanics exist. The location of the volcanics would suggest a relative slab angle of 45°, assuming subduction of more than 190 km of oceanic lithosphere or thinned European continental lithosphere and assuming that melting occurred at a depth of 100 km. Furthermore, we probably also have to correct for Badenian strike-slip or extensional movements. More to the east the slab angle becomes steeper up to 60°, considering a lower limit of 140 km subduction/underthrusting of the European lithosphere.

3. Gravity and Deep Seismic Constraints on Crustal Structures

The Bouguer gravity anomaly in the Carpathian region is characterized by negative values in the areas of the foredeep and is characterized by positive values in the Pannonian basin. The most western negative trend striking NNE is associated with the low-density sediments that fill the foredeep and Vienna basin. More to the east the trend changes strike to ENE and follows more or less the Pieniny Klippen Belt. Also, here the flexural downwarping of the European plate and the infill with partly low-density material cause the negative anomaly. These anomalies, however, are modest compared to those measured in the eastern and southern Carpathians [*Mocanu and Radulescu*, 1994]. The latter values are comparable with those measured in similar foredeep basins, such as the Apennines, Italy [*Moretti and Royden*, 1988]. A reason for the low amplitude of the absolute minimum anomaly values in the western Carpathian area is partly due to the absence of a low-density flexural root. Deep seismic lines (e.g., Figure 1b) give clear indications for a flat Moho in the western region [*Tomek et al.*, 1987; *Tomek and Hall*, 1993]. Different

scenarios are put forward to explain the dynamic cause of this feature; *Tomek and Hall* [1993] give two suggestions to explain the flat Moho: (1) precollisional relief of the Moho and (2) postcollisional creation of new Moho. Gravity models explain the absence of the root also with the soft collision of passive margin [*Lillie et al.*, 1994] or with the detachment of an oceanic slab [*Szafian et al.*, 1997]. Both latter interpretations were made for models assuming local isostasy. However, the high and low gravity anomaly couples under the mountain belts and adjacent foreland basin, respectively, result from regional compensation of the lithosphere to loading; which wavelength of response depends on the strength of the lithosphere. In this study we will analyze models similar to those of *Tomek and Hall* [1993], *Lillie et al.* [1994], and *Szafian et al.* [1997] yet incorporating the flexural behavior of the lithosphere.

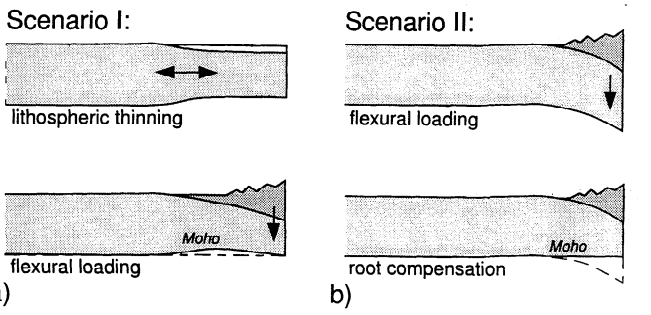

Figure 2. Cartoon illustrating two scenarios explaining the observation of flat Moho: (a) scenario I, loading a passive continental margin (PM) and (b) scenario II, compensation of flexural root by phase changes (PC).

4. Superposition of Lithospheric Processes and Their Expression in Flexural Behavior

4.1. Precollisional Processes

Modeling studies have demonstrated that collisions involving passive continental margins can generate deeper foreland basins because the water column forms an accumulation space for sediments replacing water and causes additional loading [*Stockmal et al.*, 1986]. Furthermore, the precollisional extension can also control the subsidence in a thermomechanical way. For example, subsidence as an isostatic reaction to thermal contraction is suggested to play a key role in the evolution of the Aquitaine basin, southern France, located on the northern side of the Pyrenees [*Desegaulx et al.*, 1991]. We do not expect that the thermal effect of Jurassic rifting strongly influenced the evolution of the Neogene wedge; because of the significant time gap between the two events, the temperature field would be reequilibrated [e.g., *Van Wees and Stephenson*, 1995]. However, it could have affected earlier subsidence and therefore could explain the accumulation of large amounts of Magura flysch deposits during the Paleogene, as suggested by *Roure et al.* [1994].

The supplementary subsidence associated with the extra accumulation space on passive continental margins will barely exceed 2 times the water depth. In the case of the western Carpathians, adopting reasonable paleobathymetries, the required subsidence is much more than this. Therefore additional tectonic sources, related to subduction processes, are necessary to explain the deflection. However, apart from the additional loading we also test the involvement of a passive margin in the western Carpathians as an explanation for the observed flat Moho (Figure 2a). Thinning of continental lithosphere as a mechanism for the formation of extensional basins is compensated isostatically by mantle material in a broad upward curvature of the Moho. In this study we simplify the isostatic compensation of the precollisional crustal thinning as a local (Airy) isostatic compensation and quantify the upward movement of the Moho (d_{ini}) and downward movement of the crustal surface (w_{ini}) as a function of the stretching factor (β) or crustal thinning (Δc) to $d_{ini} = \Delta c(\rho_c - \rho_w)/(\rho_m - \rho_w)$ and $w_{ini} = \Delta c(\rho_m - \rho_c)/(\rho_m - \rho_w)$ for which $\beta = c/(c - \Delta c)$ and ρ_m, ρ_c, and ρ_w are the density of mantle, crust, and water, respectively.

4.2. Postcollisional Processes

As the western Carpathians predate the eastern and southern Carpathians, flexural expressions may be affected more intensively by, for example, postorogenic erosion and superimposed processes. One of the processes that should be considered is the one that results in creating new Moho. *Tomek and Hall* [1993] propose two possible postcollisional mechanisms: (1) upward movement of the dipping position as a result of stress relaxation after the subduction ceased or slab detached and (2) a phase change to eclogite [*Austrheim*, 1994] altering former mafic lower crust to appear like unreflective mantle and forming a new seismological moho (Figure 2b).

It is unclear what isostatic effect is to be expected from slab detachment. In the Apennines, where tomographic analyses have revealed indications for slab detachment [*Wortel et al.*, 1993], flexural modeling results predict dominant effective plate boundary forces and show a still underfilled Adriatic foredeep [*Moretti and Royden*, 1988; *Royden*, 1988]. The measured Bouguer anomalies in this region show a distinct Bouguer gravity low that fits well within the predictions of the flexural model, including the low-density buoyant root. As a result, in the foredeep of the Northern Apennines no dramatic uplift is found related to slab detachment.

If in the western Carpathians slab detachment had led to unbending, because the process of slab detachment is much older than in the Apennines, the isostatic rebound would result in the creation of high mountains or exposure of high-grade metamorphic rocks, as in the Alps [*Davies and Von Blanckenburg*, 1995; *Bousquet et al.*, 1997], and large volumes of erosion products. However, this is in contrast to observations and deflection in the foredeep of the western Carpathians. Therefore stress relaxation after ceasing subduction or slab detachment cannot explain the observations of flat Moho in this region.

A phase change to eclogite is suggested by *Bois* [1992] to explain absent mountain roots from seismic lines. However, these observations were restricted to Caledonian and Variscan mountain roots. Mass balance analyses [e.g., *Laubscher*, 1988] suggest that eclogitization is responsible for the loss of crustal material in the Alps, but these studies are not verified with isostatic analyses. Apart from the effect on the seismic image of the deep crust a phase change also affects the isostatic equilibrium, because it is associated with a density

increase of 300 kg/m^3. Therefore the eclogitization process also reduces the buoyancy forces [*Richardson and England*, 1979] and consequently leads to extra subsidence. For the western Carpathians this implies, since the foredeep sediments are not younger than Miocene, that eclogitization must have been active already during Miocene and would therefore have been a synorogenic process. Without drawing further conclusions on the actual mechanism causing the flattening of the Moho, we will present the two most probable models in the flexural analysis: (1) subduction/underthrusting of passive margin (PM) and (2) a phase change in the lower crust (PC).

4.3. Controlling Basin Width Processes

Related to the possible superposition of processes, we analyze the observation of lateral changes in width along the western Carpathians. The width decreases to the southwest and increases to the east (Figure 1). Direct parameters influencing the width of a foreland basin are the strength or elastic properties of the lithosphere, controlling the flexural wavelength (Figure 3a). In addition, reduction of the topographic load would decrease the basin width. However, in this case the effect is negligible, since surface loading is small compared to the subsurface loading [*Royden*, 1993]. If slab detachment would trigger topographic uplift and erosion, this would favor widening of the foreland basin, as erosion products overfill the basin and onlap the distal boundary.

A possible explanation for a decreasing width of the foreland basin is an overall postflexural uplift (few hundred meters) including the basin and its distal foreland area (Figure 3b). A mechanism for such uplift must act on a scale larger than the flexural wavelength and must be sought for at deep crustal or lithospheric levels. Owing to this uplift, erosion would first affect the relatively soft sediments in the basin, bringing back the base level close to its original height. Because of the asymmetric shape of the basin, this process would consequently narrow the basin and accentuate the bulge area. Field indications in the west support this hypothesis. Close to Brno, beyond the distal margin of the foredeep at 350 m above sea level, remnants of marine clastic Lower Badenian sediments are found, with a depositional environment about 100 m below sea level [*Steininger et al.*, 1990], on Cadomian basement of the Bohemian Massif [*Leichmann and Hejl*, 1996]. Similar uplifted Lower Badenian sediments are found all along the distal foredeep margin between Danube and Krakow. Therefore, during the Early Badenian the accumulation space in the foredeep was larger than suggested by the current width of the basin. It is important to take this observation into account when the flexural model is constructed. A postflexural uplift of about 250 m to a maximum of 550 m is likely. The effects of postflexural uplift on the predicted isostatic response and Bouguer anomalies are discussed in more detail for profile I in section 5.

Simultaneous superposition of processes such as the interference of two systems is referred to in literature when two flexural basins interact and generate, for example, exceptionally high peripheral bulges [*Quinlan and Beaumont*, 1984]. However, in the case illustrated in Figure 3c, the interfering systems are not independently formed, but are part of the same system, slightly oblique along strike. The two curves in the profile (Figure 3c) represent projections of flexural behavior at either side of a zone marked by a change in convergence direction. A widened basin is the result of such interaction. This hypothesis is suggested for the transition area from western to eastern Carpathians, crossed by profile V (Figure 1) and discussed in section 5.4.5. in more detail.

5. Flexural Analysis of the Western Carpathians

5.1. Methodology

The flexural model is a two-dimensional finite difference simulation of flexural behavior of the lithosphere. The flexural deformation of the lithosphere is represented by a thin elastic layer overlying an inviscid fluid. Lithospheric loads are subdivided into (1) topographic loads defined by the topographic height and densities (mountain load, sediment, water, or air), (2) effective plate boundary forces, represented by a bending moment M_0 and a vertical shear force V_0, and (3) subloads represented by a top and bottom profile and a density contrast or by dynamic forces that do not contribute to the gravity field. The effective plate end is the edge of the model where boundary forces are applied. The model boundary is not assumed to be the edge of the subducting/underthrusting plate as it defines the limit where we assume the plate still carries the overlying masses. It is generally marked by a low in the Bouguer gravity anomaly. The processes active on the

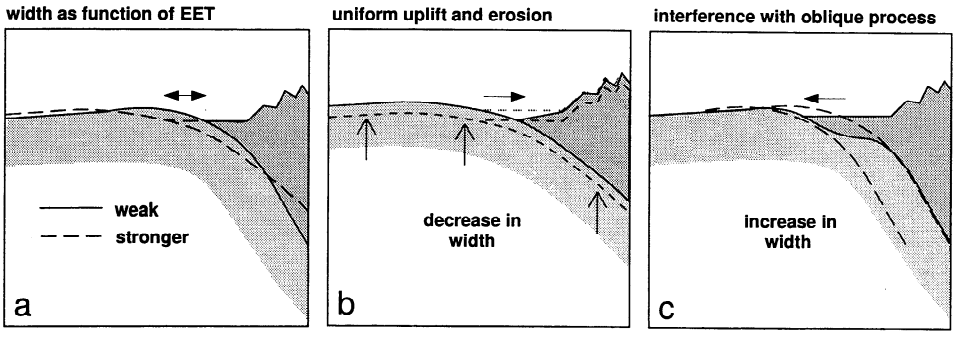

Figure 3. Cartoon illustrating three factors controlling widths of foreland basin: (a) effective elastic thickness of the plate, (b) basin erosion due to uniform uplift, and (c) interacting flexural processes (see text for discussion).

deeper part of the plate are represented by the effective plate boundary forces.

Preorogenic crustal thinning is incorporated in the flexural model. The heights of the resulting water- and mantle columns are isostatically balanced. Except for some details the model is similar to that applied for the Pyrenees [*Zoetemeijer et al.*, 1990; *Millan et al.*, 1995] and Romanian eastern and southern Carpathians [*Matenco et al.*, 1997].

In the model we differentiate six different densities (Table 1) that can form all different density contrasts. The densities are chosen to be uniform along the different profiles. All density bodies that deviate from the initial model contribute to the simulated Bouguer gravity anomaly and are compared with the Bouguer anomaly data. This method underestimates the possible (positive) effect of plate boundary forces on the gravity anomaly, since the forces are not represented by density contrasts. However, the effect is restricted to the flank of the minimum low opposite to the flank under the foredeep [*Royden*, 1993].

5.2. Basement Depth Data

The flexural model is applied to five profiles crossing the western Outer Carpathians. To constrain basement depth, the profiles are chosen to be parallel to (deep) seismic lines. Profile I is the most southwestern profile and is parallel to the 8HR/86 line that has recorded reflections up to 16 s [*Tomek and Hall*, 1993]. A detail of this line is shown in Figure 1b. The line is depth converted down to 40 km. Profile II is parallel to the T240 reflection line, which is used for studying the upper 20 km of crust. The wide-angle trans-Carpathian reflection line KII is used to study the complexities at the Moho [*Mayerova et al.*, 1983]; profile III is constrained in the Polish part by an unpublished seismic line in which depth conversion is down to 6 km. In the south the profile is parallel to the 2T deep seismic line recording reflections up to 16 s [*Tomek*, 1993]. Profile IV is based on the interpretation of the geotraverse of the Polish Carpathians passing along the cities of Krakow and Zakopane [e.g., *Lefeld and Jankowski*, 1985]. Profile V corresponds to the Jankowce-Paszowa-Kuzmina-Cisowa line [*Wdowiarz and Jucha*, 1981; *Wdowiarz*, 1983]. Indications for the depth of basement under the foredeep along this profile are obtained from *Zytko et al.* [1989]. Furthermore, apart from the seismic data a total of 21 wells constrain the depth of the basement in the study area (Figure 1) [e.g., *Karnkowski*, 1986]. The depth to Moho is derived from *Horvath* [1993].

Table 1. Parameters Adopted in Flexural and Gravity Modeling

Parameter	Value
Density of water	1000 kg/m^3
Density of infill	2450 kg/m^3
Density of surface load	2640 kg/m^3
Density of crust	2900 kg/m^3
Density of mantle	3200 kg/m^3
Density for Bouguer correction	2670 kg/m^3
Young's modulus	7.0 10^{10} N/m^2
Poisson's ratio	0.25

5.3. Gravity Data

In this paper we use Bouguer gravity data from the Bouguer map published by *Tomek* [1988]. In Poland the data set is extended with data from *Krolikowski and Petecki* [1995]. When preparing a regional gravity map crossing the borders of various countries, one encounters differences in methods for deriving the Bouguer anomaly from the measured gravity field. Generally applied in eastern Europe [e.g., *Lillie et al.*, 1994; *Szafian et al.*, 1997] is a Bouguer anomaly computed for the normal Helmert gravity formula in the Potsdam system [*Torge*, 1989]. For the preparation of the new gravimetric map by *Krolikowski and Petecki* [1995] the editors decided to recalculate the gravity anomalies after facing problems in combining analyses and exchanging data during international collaborations. Land gravity values were recalculated in the IGSN 71 system (International Gravity Standardization Net 1971). Furthermore, the GRS 80 (Geodetic Reference System 1980) formula was applied, based on the geocentric Earth ellipsoid [*Torge*, 1989], and the density for the Bouguer correction for material above sea level was set to 2670 kg/m^3 instead of 2550 kg/m^3. As a result, the difference between the map of *Tomek* [1988] and the gravimetric map of Poland by *Krolikowski and Petecki* [1995] is a constant value of approximately 20 mGals. Polish data are therefore shifted with a constant value of 20 mGals. This uncertainty in the correctness of the reference normal field keeps us from drawing firm conclusions on possible mechanisms for an overall uplift. Further on in this paper we will come back to this.

5.4. Model Results

The flexural model contains a number of free parameters that influence the results in a different way. *Royden* [1988] showed this in detail for the flexural modeling of the Apennines. In this study we present the sensitivity of the model for different assumptions in as detailed a way as possible, examining different parameters for each profile. When presenting profile I, the effect of the overall uplift of the system is introduced. When presenting profile II, we explore the model sensitivity for the different scenarios (PM and PC) that explain flat Moho. Profile III is used to quantify the control of lateral weakening of the lithosphere by varying the effective elastic thickness (EET) along the profile, especially in the area of maximum bending. In profile V the boundary conditions play an important role, and therefore when presenting the modeling results for profile V, the boundary conditions are discussed in more detail.

5.4.1. Profile I. This is the most western profile (Figure 4, see Figure 1 for location). It is NW-SE oriented, a major part crossing the Bohemian Massif, and it traverses the Neogene foredeep close to Brno. Here the Carpathian thrust wedge is only outcropping over 25 km. Although seismic reflection data give clear indications for the existence of Magura flysch units under the Vienna basin [*Tomek and Hall*, 1993], we do not extend the model farther SE of the Vienna basin. We assume that southeast of the Vienna basin the subducted European lithosphere does not isostatically support the surface structures, but these are supported by the Central Carpathian – North Pannonian lithosphere fragment. In other words, sur-

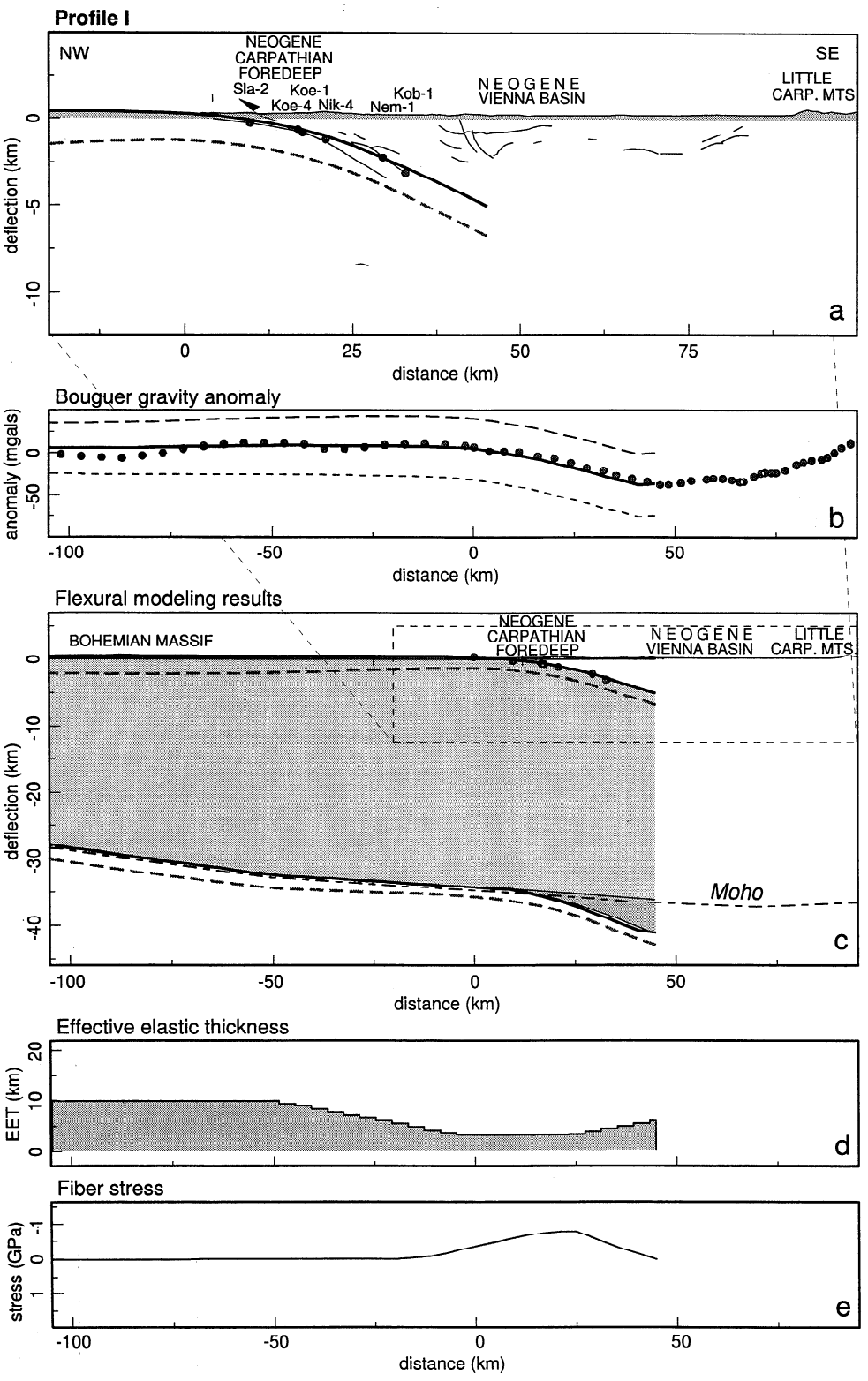

Figure 4. Cross section of profile I, see Figure 1 for location. (a) NW-SE oriented profile. Thin lines are depth indications from 8HR/86 seismic reflection line, Circles show well indications for depth to basement, bold solid line shows best fitting flexural model prediction, and shaded dashed line shows model response without incorporating overall uplift mechanism. (b) Bouguer gravity anomaly. Circles show Bouguer gravity data according Helmert formula, bold solid line indicates best fitting Bouguer anomaly prediction (no density contribution from process of uplift), long-dashed line indicates Bouguer anomaly prediction for model incorporating positive density contribution of uplift, and short-dashed line indicates Bouguer anomaly prediction for model incorporating negative density contribution of uplift. (c) Crustal profile of flexural modeling results. Dark-shaded root indicates subload simulating phase change (PC); irregular dashed line indicates actual Moho profile. (d) Lateral distribution of effective elastic thickness (EET) for best fitting model. (e) Fiber stress σ_{xx} for best fitting model (negative values for tension at surface).

face loading southeast of the Vienna basin is not transmitted to the subducting slab. However, subsurface loads, representing the slab-pull force, may be still active and are projected in the model to the boundary conditions (vertical shear force V_0 and bending moment M_0). We have defined the edge of the flexural model at 45 km, which is under the western margin of the Vienna basin (Figure 4a) and coincides with the minimum in the Bouguer gravity anomaly.

The foredeep is steeply dipping to the SE. Relatively low effective elastic thicknesses (EETs) can explain the sharp bending of the lithosphere. The strength of the European lithosphere is simulated locally by an EET of only 3.5 km. The low in the EET profile (Figure 4d) coincides well with the maximum bending of the plate (Figure 4e). These applied bending stresses may extend beyond the maximum stress that the lithosphere can carry and consequently result in brittle failure at the surface and ductile deformation in the lower crust, which will subsequently weaken the lithosphere. Although this mechanism is not incorporated in the flexural model the process may be simulated with the assumption of weakness zones in the model.

The observation of flat Moho is explained and simulated with a phase change in a zone as large as the flexural root (Figure 4c). The buoyant root of the crust, plunging in the mantle, is counterbalanced by a subload body with a 300-kg/m^3 density contrast. The positive effect of the subload on the Bouguer gravity anomaly is incorporated. The plate boundary forces, representing the subduction/underthrusting processes beyond the southeastern model edge, are small: $M_0 = 0$. N and $V_0 = 2.0\ 10^{11}$ N/m. Such vertical shear force resembles the mass of a 10-km-long, 20-km-thick slab with 100 kg/m^3 density contrast.

Topographic elevations in the western Carpathians are low, generally not exceeding 330 m, decreasing to ~250 m in the Vienna basin. An exception is the Male Karpati (495 m) at 100 km SE, but this part is not incorporated into the model, since it is not loading the European lithosphere. At the foreland side, however, the Bohemian Massif is generally 400 m above sea level and maximally 645 m at -87 km NW. Since remnants of Miocene deposits are found beyond the distal margin of the foredeep on the Bohemian Massif, we assume that the area is uplifted a few hundred meters after subduction/underthrusting. As we mentioned in section 4.3. the uplift is possibly an overall uplift in the region larger than the flexural wavelength. On the basis of the topographic elevation of the foreland we have incorporated a continuous subload causing an uplift of 250 m in the belt, increasing to 300 m near Brno and to 540 m in the Bohemian Massif. In Figures 4a and 4c we show the contrast between the model results taking the uplift into account and the consequences of not incorporating such a postcollisional process. Figure 4b presents the simulated Bouguer gravity anomaly matching the observed Bouguer gravity anomaly, when forces produce the uplift. Figure 4b also gives the predictions for the subload being (1) a thermal uplift (isostatic response to density decrease due to thermal expansion) causing a negative shift in the Bouguer anomaly and (2) an nonisostatically compensated uplift, causing a positive shift in the Bouguer anomaly. The possible processes for explaining the uplift and Bouguer anomalies are discussed below in more detail.

5.4.2. Profile II. This profile is located about 100 km along strike, east of profile I (Figure 5, see Figure 1 for location). It is directed NNW-SSE and crosses the elevated Rhenohercynian flysch units of the foreland region east of the Bohemian Massif. Here topography forms the highest elevated part of the distal foreland at ~450 m above sea level, where the topography is ~330 m in the foredeep. The sharp topographic contrast between the basement of the distal foreland and the foredeep indicates again postcollisional erosion of parts of the foredeep. The assumed uplift is incorporated into the modeling by a continuous subload of 450 m high between the belt (65 km SSE) and distal foreland (–75 km NNW).

The topographic load of the belt, about 500-600 m above sea level, is carried by the subducting/underthrusting European lithosphere up to 10 km NNW of the Pieniny Klippen Belt (75 km SSE) (Figure 5a). The location of the effective plate boundary (65 km SSE) coincides with the minimum in the Bouguer gravity anomaly (Figure 5b). Again, the foredeep is steeply dipping and is explained by a weakness zone (Figure 5d) coinciding with the place of maximum flexural bending (Figure 5e). EET decreases locally to 5.0 km. The subduction/underthrusting processes are modest and similar to profile I: $M_0 = 0$. N and $V_0 = 2.0\ 10^{11}$ N/m.

In order to explain the flat Moho, both scenarios of passive margin subduction (PM) and of phase change (PC) are applied. The passive margin configuration is simulated in the model by including an asymmetric paleowater depth profile with its onset at sea level located 25 km SSE, deepening to the SSE down to ~1500 m at the effective plate boundary (Figure 5c). The water column is isostatically balanced by thinning of the crust. Although for the PM scenario a fit is obtained for the deflection and gravity anomaly, the Moho is too much thinned and curved upward (Figure 5c). For the PC scenario a similar approach is followed as in the modeling of profile I. The buoyant crustal root is balanced by a root with positive density contrast of 300 kg/m^3. Although the modeling of Moho and basin deflection is successful for the PC scenario, the gravity does not fit well. Best fits are presented in Figure 5b.

Generally, if a fit is possible, application of the two scenarios can predict similar basin deflections, gravity anomalies, and Moho profiles. Hence solely on the basis of these data the flexural modeling cannot distinguish the two scenarios for explaining flat Moho. In fact, this is not surprising; the observed deflection requires similar downpulling forces. Since these forces are purely controlled by density changes that are of the same order (both contrasts of crust/mantle and phase change are 300 kg/m^3), they will also produce similar anomalous bodies. Although the depths of the different density contrasts are different (initially above the Moho for the PM scenario and concentrated in the root below the Moho for the PC scenario), the effect on the Bouguer gravity anomaly is hardly different. The two scenarios presented here form the end-members of a range of possible models. Additional data such as paleowater depths are necessary to further constrain the model.

5.4.3. Profile III. This profile is located 90 km farther to the east, almost parallel to profile II (Figure 6, see Figure 1

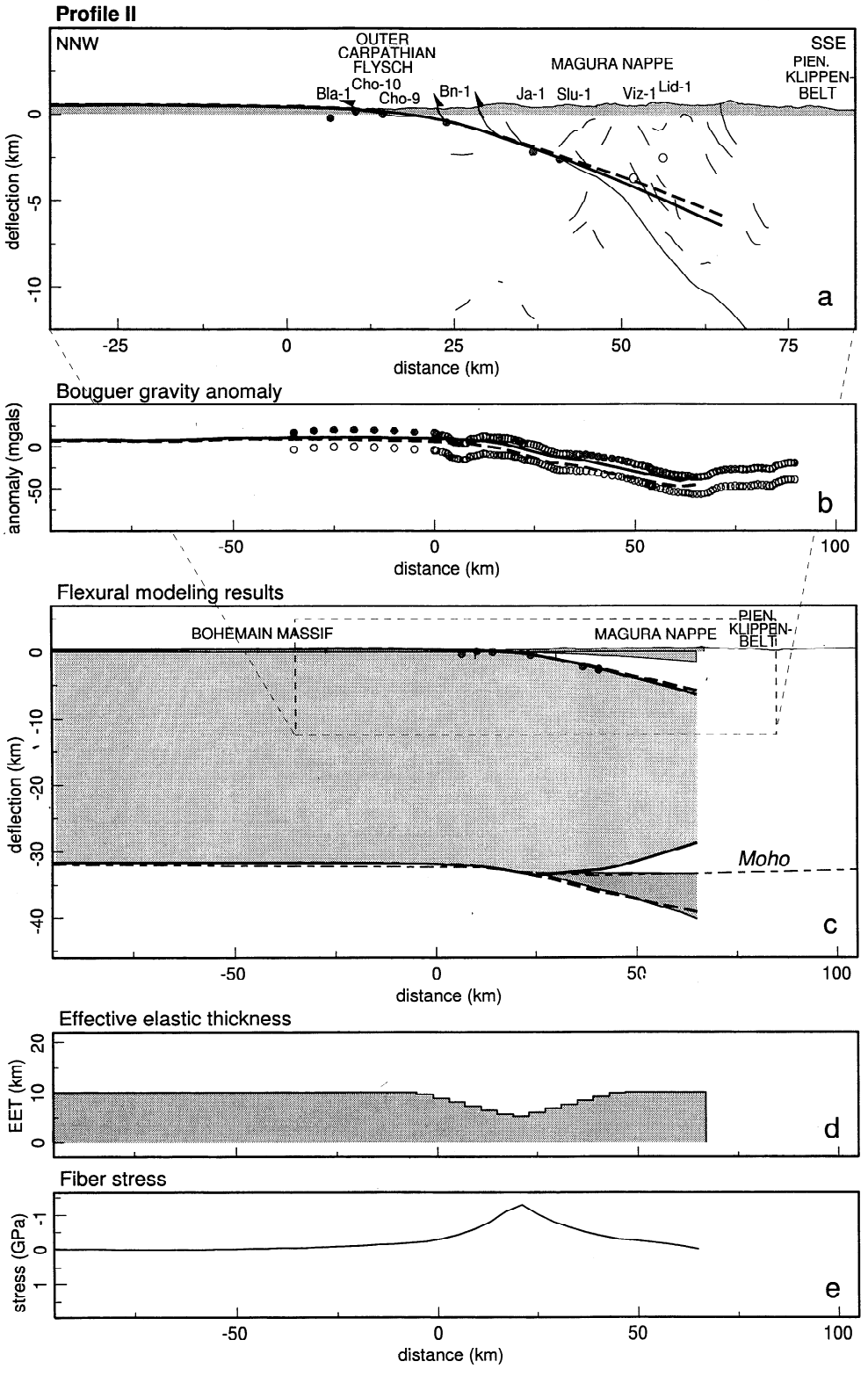

Figure 5. Cross section of profile II, see Figure 1 for location. (a) NNW-SSE oriented profile. Thin lines are depth indications from T240 seismic reflection line; Circles show well indications for depth to basement, bold solid line shows best fitting flexural model prediction for the PM scenario, bold dashed line shows best fitting flexural model prediction for the PC scenario. (b) Bouguer gravity anomaly. Solid circles show Bouguer gravity data according to Helmert formula, open circles show Bouguer gravity data according to IGSN 71 system, and bold lines show best fitting Bougeur anomaly predictions for scenarios PM and PC, as in Figure 5a (no density contribution from process of uplift). (c) Crustal profile of flexural modeling results. Dark-shaded root indicates subload simulating phase change, irregular dashed line indicates actual Moho profile. (d) Lateral distribution of effective elastic thickness for best fitting models. (e) Fiber stress σ_{xx} for PM scenario (negative values for tension at surface).

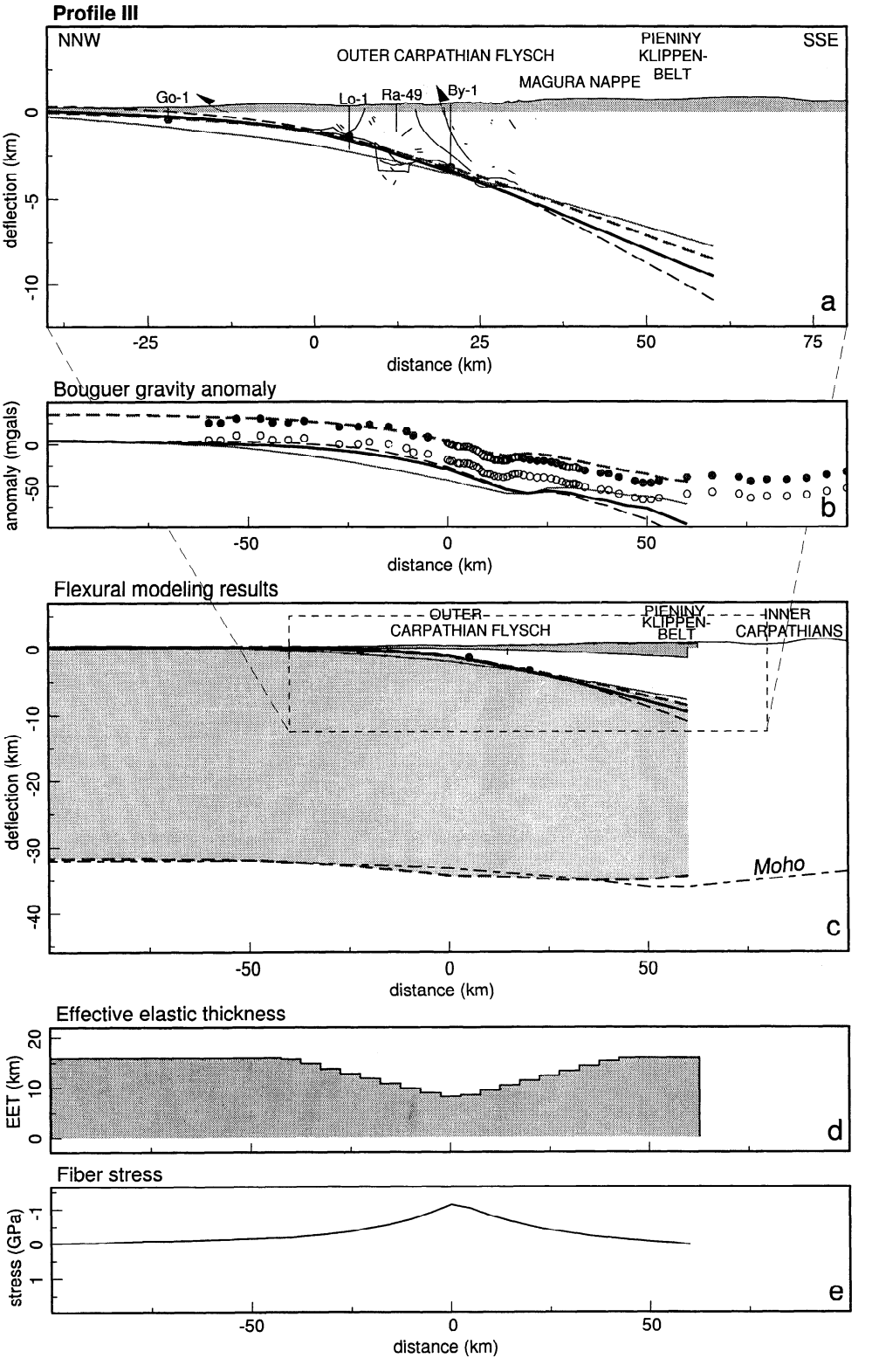

Figure 6. Cross-section of profile III, see Figure 1 for location. (a) NNW-SSE oriented profile. Thin lines are depth indications from 2T seismic reflection line, circles show well indications for depth to basement, bold solid line shows best fitting flexural model prediction not incorporating density contribution from process of uplift, shaded dashed line shows best fitting flexural model prediction incorporating positive density contribution from process of uplift, dashed line shows flexural model prediction for constant EET of 8 km, and thin shaded line shows flexural model prediction for constant EET of 16 km. (b) Circle indications as in Figure 5b and line indications as in Figure 6a. (c) Crustal profile of flexural modeling results. Dashed shaded line at Moho level shows flexural model prediction of Moho for the PM scenario; irregular dashed line shows actual Moho profile. (d) Lateral distribution of effective elastic thickness for best fitting models. (e) Fiber stress σ_{xx} for PM scenario (negative values for tension at surface).

for location) and parallel to the 2T seismic line. The topographic elevation of the distal foreland is lower compared to profiles I and II. A constant subload causing an uplift of 250 m is assumed along this profile from the Inner Carpathians to ~100 km NNW (Figure 6). A flat Moho is simulated according the PM scenario similar to profile II, assuming a paleowater depth profile with the onset at 0 km and deepening to ~1400 m below sea level at the effective plate boundary (Figure 6c). The effective plate boundary is assumed to be at 10 km SSE of the Pieniny Klippen Belt that is outcropping 20 km SSE of the Polish/Slovak border. The Bouguer gravity minimum also corresponds to the location of the Pieniny Klippen Belt (Figure 6b). The boundary conditions slightly increase in importance in respect to profiles I and II: $M_0 = 0$. N and $V_0 = 3.5\ 10^{11}$ N/m.

In the zone of maximum bending the EET decreases from 16 km to 8 km (Figure 6d). In order to compare the results of the model incorporating local weakening with that of uniform elastic plates with 8 and 16 km EET, we present these latter simulations too (Figures 6a-6c). We can only determine EET in flexural curved areas. In areas where bending is close to zero, the model predictions are almost insensitive for the assumed EET; with only little effect on the deflection the EET can also be smaller or larger. This is true for all profiles presented here and all flexural analyses presented earlier. However, in the bent area the EET strongly controls the deflection in the basin and therefore also the weakness zones. The weakening may be due to yielding of the lithosphere under applied flexural bending stresses, as supported by the modeling results.

The deflection in the foredeep is constrained by seismic data at the Polish side of the 2T line. Farther to the SSE, modeling results predict basement at 8 km under the Pieniny Klippen Belt and 10 km at the effective plate boundary (Figure 6a). This means that the European lithosphere dips maximally 11° to the SSE in this area. Neogene volcanics crop out close to the profile about 120 km SSE, 60 km SSE of the effective plate boundary. If this volcanism is caused by melting of the European lithosphere at 100 km depth, the slab should dip further to an angle of 60° to reach this depth within this short distance. The 2T deep seismic line, crossing the Slovak Outer Carpathians, suggests a steeply dipping European lithosphere to 20 km depth under the Pieniny Klippen Belt and 35 km depth at 30 km SSE of the border [*Tomek*, 1993]. These values may be overestimated, because the depth conversion is carried out for a single velocity of 6 km/s. In this way the depths of shallow reflectors can be 40% overestimated, because waves travel through foreland basin deposits and flysch units, which have much lower seismic velocity.

5.4.4. Profile IV. This profile is N–S directed and is located close to the meridian of 20° longitude near Krakow (Figure 7, see Figure 1 for location). The area has been studied intensively by geological mapping [*Slaczka*, 1975] (see also references of, e.g., *Birkenmajer* [1985], *Oszczypko et al.* [1989], *Poprawa and Nemcok* [1989], and *Zytko et al.* [1989]), and subsurface geometry is constrained by seismics and boreholes. To the north on the European foreland the profile crosses obliquely the NW-SE oriented Mesozoic Polish trough rift system, with its depocenter in the Miechów depression, which is filled with Upper Cretaceous limestones [*Oszczypko et al.*, 1989]. Since the profile crosses the zone only in the distal part of the subduction/underthrusting system, the influence of the possible different mechanical properties of this zone is only expected in the area of the peripheral bulge and is, because of low flexural bending stresses, difficult to quantify. According to *Oszczypko et al.* [1989] the basement under the Magura unit, especially at the border between the Magura and Silesian unit, shows normal faults with offsets of the order of 1000 m (Figure 7a). These structures are not directly associated with the Mesozoic extension, because they are SW-NE directed. They are documented in Polish literature as dislocations or crustal fractures [*Oszczypko and Slaczka*, 1985; *Bojdys and Lemberger*, 1986; *Oszczypko et al.*, 1989]. They played a minor role during the Cretaceous, but during the collision they seem to control the location of the most external basal ramp of the Magura flysch unit. This relationship between the location of the basal ramp of the Magura flysch unit and the basement faults also seems to occur more to the west in profile III and IV. A possible reactivation of the faults in Badenian time would agree well with the brittle failure of the European lithosphere because of applied flexural bending stresses; the position of the faults coincides with the assumed low EET values (5 km, Figure 7d) and the position of maximum bending (Figure 7e). In section 6 we will discuss further the relation between normal faulting, flexural bending stresses, and elastic behavior.

The topographic elevation has its minimum of 213 m above sea level at the distal margin of the foredeep. The foredeep and distal foreland show an average elevation of 300 m with a maximum of 342 m at 130 km N. Also, for profile IV we assumed a subload causing 300 m overall uplift of the subduction/underthrusting system from the Inner Carpathians to the distal foreland far to the north. The Bouguer gravity anomaly and the location of the Pieniny Klippen Belt coincide closely with the effective plate boundary 10 km north of Zakopane (Figure 7b). Flat Moho is simulated with the PC scenario, replacing the buoyant crustal root with a subload density contrast of 300 kg/m^3. The model results indicate that the effective plate boundary conditions increase in importance toward the east: $M_0 = 0$. N and $V_0 = 5.0\ 10^{11}$ N/m, relative to the other profiles.

5.4.5. Profile V. This profile is the most easterly located profile (Figure 8, see Figure 1 for location). It crosses the thrust front about 200 km along strike, east of profile IV. It is oriented NE-SW and passes close along the Ukrainian border. The basin is much wider than to the west, and the Outer Carpathian thrust belt also reaches its maximum width in this area. The Magura flysch unit decreases again in importance, and Dukla, Silesian, and Skole units dominate the thrust wedge of the Outer Carpathians. The gravity minimum is no longer following the location of the Pieniny Klippen Belt but deviates to the northeast and coincides with the boundary between the Silesian and Skole overthrust units. To the east the subduction/underthrusting system is clearly controlled by the NNW trending Tornquist-Teisseyre zone, the transition zone from the European to east European platform. Obviously, this part of the foreland is dominated by the transition from the E-W trend of the Carpathians, overthrusting west

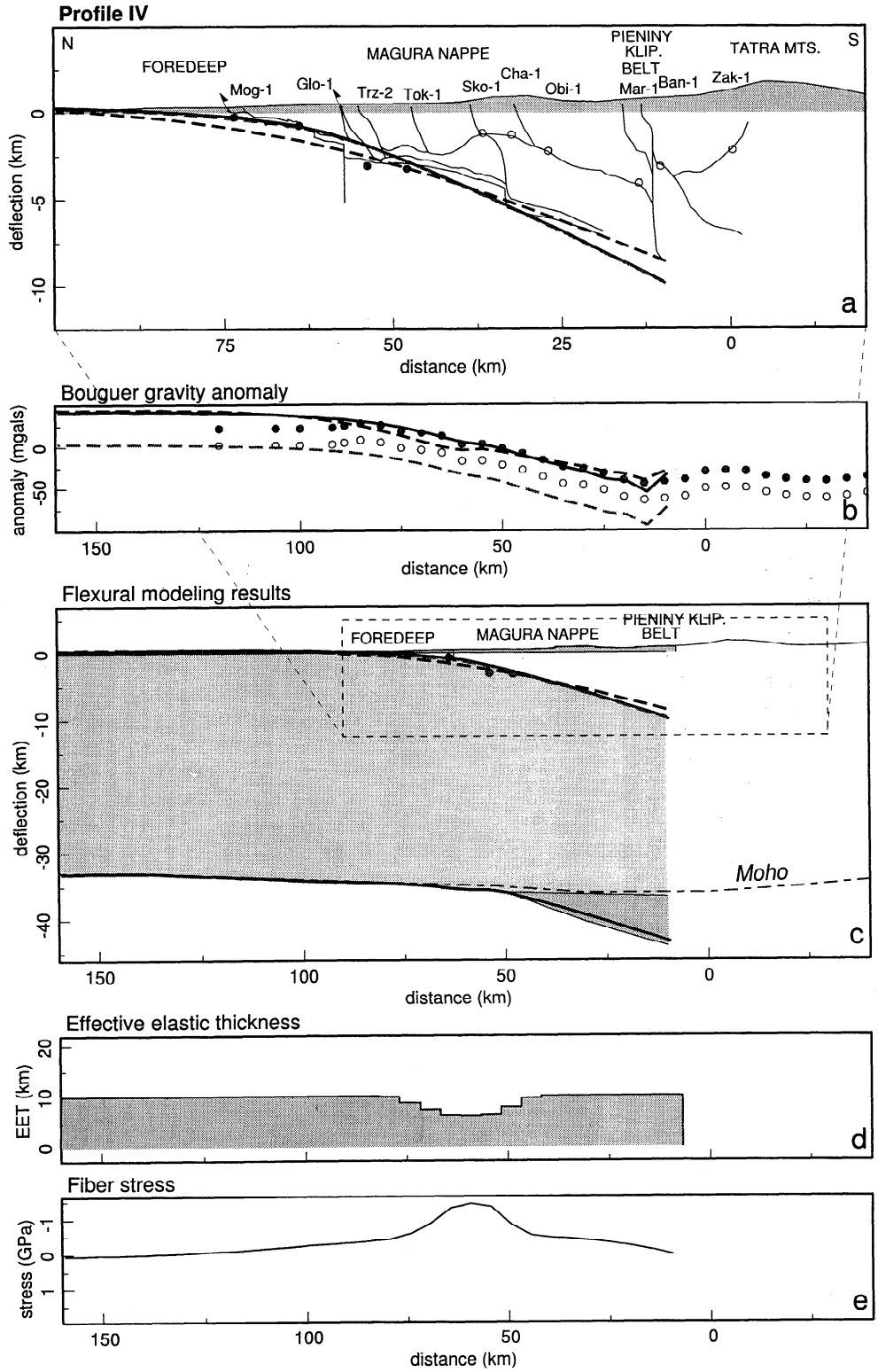

Figure 7. Cross section of profile IV, see Figure 1 for location. (a) N-S oriented profile. Thin lines are depth indications from Krakow-Zakopane seismic reflection line, solid circles show well indication for depth to basement, bold solid line (covered by dashed shaded line) shows best fitting flexural model prediction incorporating positive density contribution from process of uplift, dashed shaded line shows best fitting flexural model prediction not incorporating density contribution from process of uplift, and dashed line shows flexural model prediction for constant EET of 10 km. (b) Circle indications as in Figure 5b and line indications as in Figure 7a. (c) Crustal profile of flexural modeling results. Bold line at Moho level shows flexural model prediction of deflection for the PC scenario (deflection minus root gives predicted Moho depth), dark-shaded root shows subload simulating phase change, and irregular dashed line shows actual Moho profile. (d) Lateral distribution of effective elastic thickness for best fitting models. (e) Fiber stress σ_{xx} for best fitting models (negative values for tension at surface).

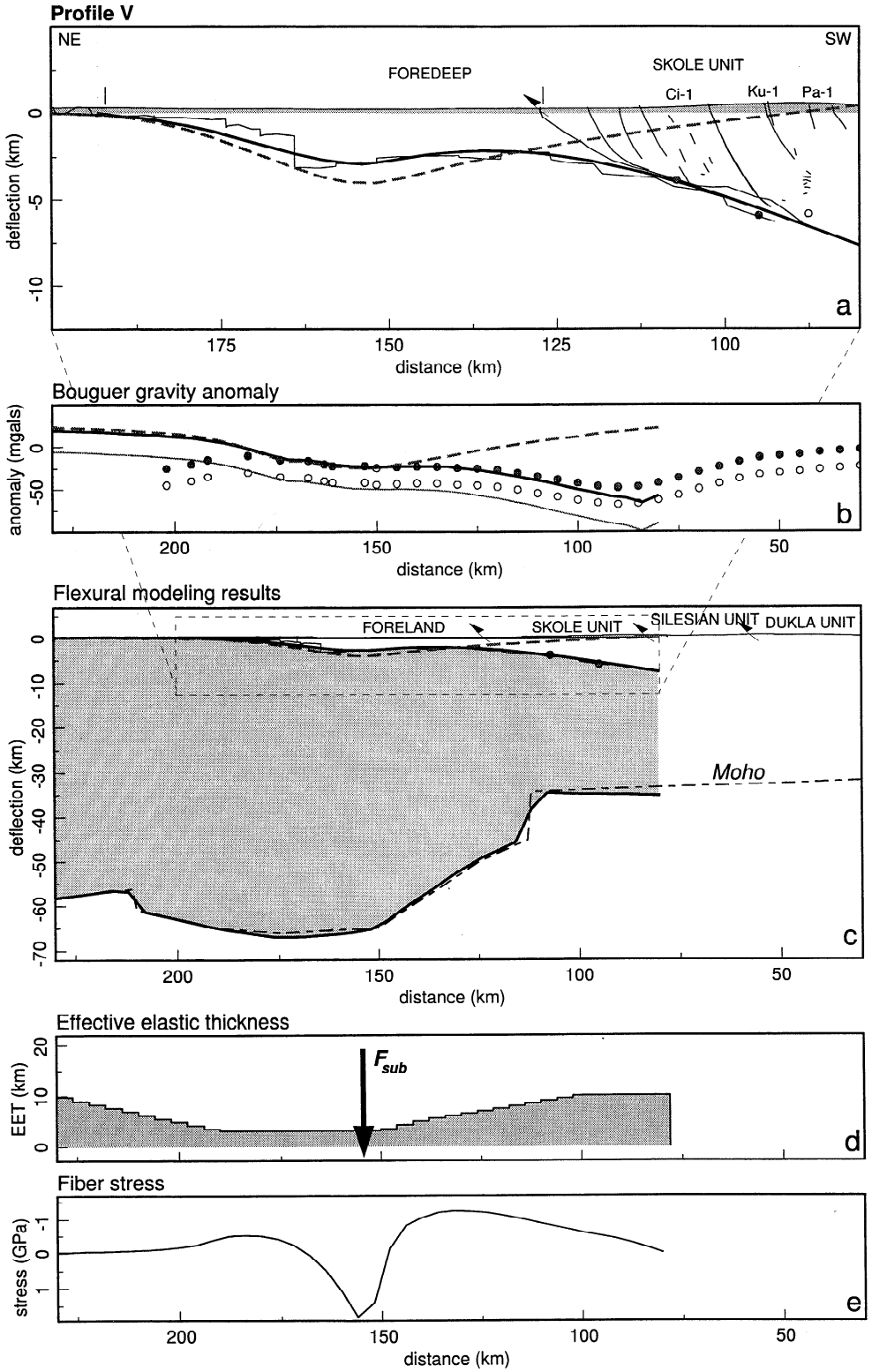

Figure 8. Cross section of profile V, see Figure 1 for location. (a) NE-SW oriented profile. Thin lines are depth indications from Krakow-Zakopane seismic reflection line, solid circles show well indications for depth to basement, bold solid line shows best fitting flexural model prediction incorporating positive density contribution from process of uplift, and dashed shaded line shows model prediction for simulation without plate-boundary forces. (b) Circle indications as in Figure 5b and line indications as in Figure 8a. Thin shaded line shows Bouguer gravity simulation for best fitting model, without density contribution from process of uplift. (c) Crustal profile of flexural modeling results. Note the different vertical scale relative to Figures 4c-7c. Irregular dashed line shows actual Moho profile (crossing anomalous thick crust of TT zone). (d) Lateral distribution of effective elastic thickness for best fitting model. Arrow shows location of subload force simulating lateral interaction of oblique process. (e) Fiber stress σ_{xx} for best fitting model (negative values for tension at surface). Note the high compressional stresses close to the subload force (F_{sub}).

European lithosphere, to the NW-SE trend of the Carpathians, approaching the east European platform.

The average topographic height along this profile reaches its maximum near the Slovak-Polish border (50 km NE, Figure 8). NE of the thrust front the topography rapidly decreases to about 230 m and increases again locally at the distal margin of the basin (300 m above sea level at 190 km NE). We incorporated in the modeling a continuous subload creating an uplift of 225 m above sea level. The numerous normal faults cutting the foreland basement are here oriented NW-SE and correspond to the TT zone and Mesozoic rifting [*Oszczypko et al.*, 1989]. Although the flexural basement curvature is somewhat disturbed because of block faulting, it shows a clear local high and low in the foredeep (Figure 8a). Along strike the displacement along the normal faults becomes more dominant to the SE in the eastern Carpathians. Low EET values cannot explain the short-wavelength curvature of the lithosphere under the foredeep; active forces need to be applied to simulate such lithosphere behavior. Although the system is still dominated by the E-W trend of the western Carpathians, it is also affected by the east European system. In order to account for the interaction of the oblique subduction/underthrusting system of the eastern Carpathians, we applied a single downpulling force of 1.0 10^{12} N/m at 154 km NE (Figure 8d). This force is relatively high and even higher than the subduction force applied to the effective plate boundary at 80 km NE (8.0 10^{11} N/m). Obviously, the 2–D modeling is incapable of modeling the details of these complex settings, requiring 3–D modeling [e.g., *Van Wees and Cloetingh*, 1994].

We assume that the normal faults are reactivated by the applied flexural bending stresses. If the bending stress exceeds a critical value, the lithosphere can yield its complete strength, and as a result, stresses can no longer be transmitted laterally. In order to test such a situation, we have modeled a scenario with boundary conditions put to zero (Figure 8a-8c). From this test it is clear that the subduction/underthrusting processes are dominant, which indicates that underthrusted European lithosphere is still strong enough to transmit the slab-pull force to the foreland in spite of the weakening and crustal sutures. In section 6 we will analyze the model results for simplified elastic-plastic behavior of the European lithosphere in order to validate and examine the limitations of a pure elastic model.

6. Lithosphere Rheology: Consequences for the Elastic Plate Predictions

The European continental lithosphere under the western Carpathians is very diverse in age, crustal thickness and temperature. Therefore the mechanically strong part of the lithosphere based on depth-dependent (brittle-elastic-ductile) rheology of crust and mantle is supposed to vary similarly [*Lankreijer et al.*, 1997]. As we summarize the predictions of the flexural modeling, we must conclude that such variation in EET relative to age, crustal thickness, or temperature is lacking. However, the flexural modeling clearly shows the control of plate deformation in the predictions of EET. We have mentioned earlier that the flexural model can only constrain EET in flexural curved areas and that in areas where bending is close to zero the model response is insensitive for the assumed EET. In other words, we can hardly extend the predicted EET values to nondeformed areas. *Burov and Diament* [1995] have drawn similar conclusions; in regions of intense deformations, with curvature smaller than 10^3 km, the EET can be reduced by a factor of 2-5 because of inelastic deformation (brittle failure and ductile flow). However, the authors do not correct the EET values obtained from analyses in highly bent areas [e.g., *Royden*, 1988, 1993]. EET estimates from *Okaya et al.* [1996] for the Swiss Alps are inferred from synthetic rheological profiles constructed on the basis of local geophysical data. Weakening of the lithosphere due to flexural bending is therefore not incorporated, contributing to differences between their values and inferences from flexural modeling predictions in the area.

From our analyses we conclude that the European continental lithosphere under the western Carpathians is intensively deformed, reflected in generally low predicted EET values. A problem to be considered now is to judge how intense the deformation is and whether the assumption of elastic deformation is still valid.

A first step in extending the model from pure elastic deformation (Figure 9a) to depth-dependent multilayered decoupled rheology (Figure 9b) is setting an upper bound for the applied elastic deformation (Figure 9c). In this approach we follow *Turcotte and Schubert* [1982]: given the relations for a single elastic plate, with the vertical axis represented by the parameter y, the horizontal axis along the profile represented by the x, the flexural bending stress σ_{xx}, Young's modulus E, Poissons's ratio ν, elastic strain ε and deflection w:

$$\sigma_{xx} = \frac{E}{1-\nu^2}\varepsilon_{xx} \quad \wedge \quad \varepsilon_{xx} = -y\frac{d^2w}{dx^2} \tag{1}$$

The flexural bending stress or fiber stress [*Ranalli*, 1987] in an elastic plate is given by

$$\sigma_{xx} = \frac{-E\,y}{1-\nu^2}\frac{d^2w}{dx^2} \tag{2}$$

Assuming an elastic-plastic rheology for the bending of the plate, the stress increases linearly with distance y (in depth) from the center of the plate ($y = 0$). The plate bends elastically until the stress at the surface becomes sufficiently large that yielding occurs. The yield stress may be simplified to $\sigma^* = \sigma_{xx}$. From these relations and using the expression for the bending moment $M(x) = -D(x)\, d^2w/dx^2$, one can determine the bending moment M_{on} corresponding to the onset of plasticity for $y = \frac{1}{2}h$ (h = EET) and M_c the critical bending moment for the situation of entire yielding for $y = 0$: $M_{on} = -\sigma^* h^2/6$ and $M_c = -\sigma^* h^2/4$ (for details see *Turcotte and Schubert* [1982, section 7.11]).

Figure 10 shows the fiber stresses σ_{xx} of the modeled profiles (also plotted in Figures 4-8e) relative to the distance from the plate edge, including indications for the onset of yielding at $\sigma^* = 1$ GPa and entire yielding at an extrapolated fictive stress level of $\sigma_{xx} = 1\frac{1}{2}\,\sigma^*$. Yielding is suggested for profiles IV and V, and even complete yielding may occur at the local depression in profile V.

7. Dynamic Process for Postcollisional Uplift

An overall postcollisional uplift (Figure 3b) of the European foreland in vicinity of the western Carpathians is pre-

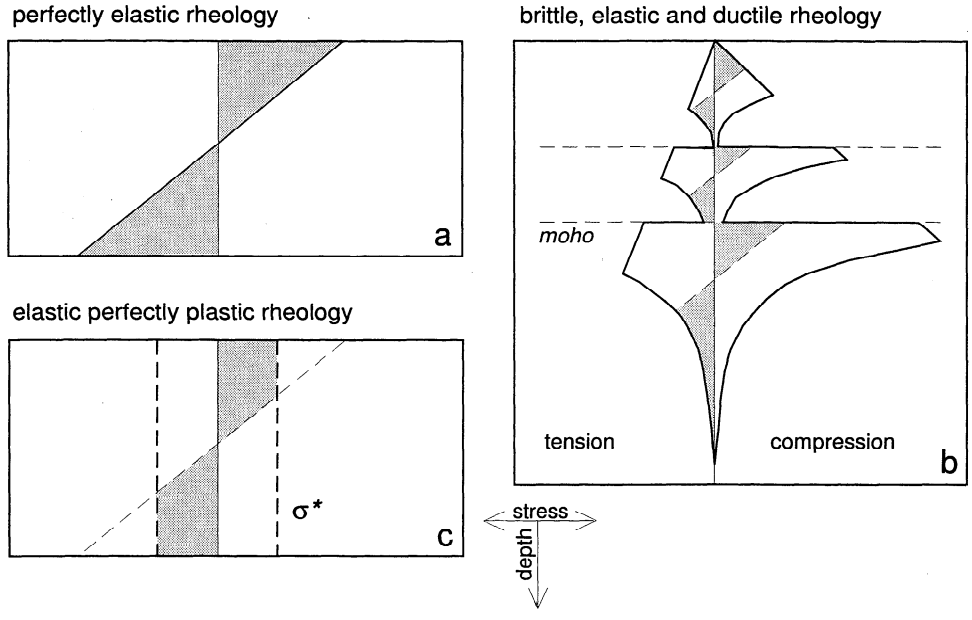

Figure 9. Cartoon showing different rheological models of continental lithosphere. (a) Pure elastic behavior. (b) Depth-dependent brittle-elastic-ductile rheology. (c) Elastic perfectly plastic rheology of simplified continental lithosphere.

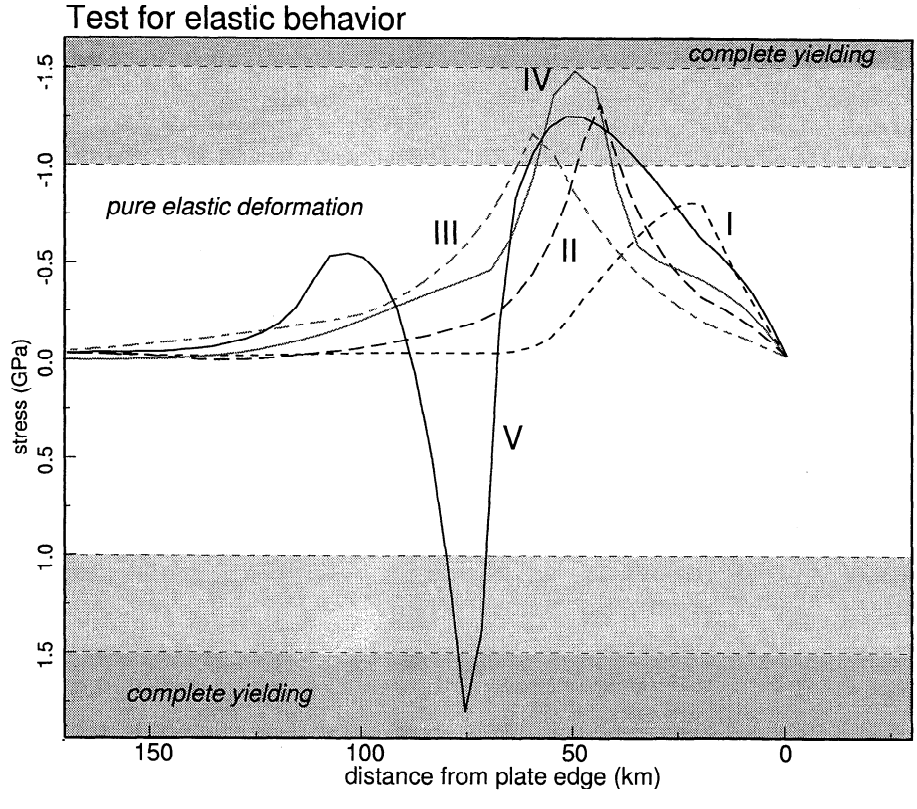

Figure 10. Predicted variations of fiber stress σ_{xx} as a function of distance from the plate edge for profiles I, II, III, IV, and V (negative values for tension at surface). Light-shaded areas show onset of plasticity; dark-shaded areas show perfect plastic deformation for yield stress $\sigma^* = 1$ GPa (no stresses can be transferred through this zone). See text for discussion.

dicted along all profiles. The uplift varies from 300 m near Brno to 540 m in the Bohemian Massif, 450 m in the Rhenohercynian flysch units east of the Bohemian Massif, decreasing again to about 250 m, 300 m, and 225 m along profiles III, IV, and V, respectively. Recent uplift is also recognized in the Viena basin, and foreland basin sediments in the eastern Alps are passively elevated to 700 m above sea level [*Andeweg and Cloetingh*, 1998].

The mechanism of uplift is probably a very regional process. It is possibly associated with the inversion of the intraplate stress field [*Horvath and Cloetingh*, 1996] or associated with the thermal development in the Pannonian area (5–0 Ma), because the uplift also seems to be accompanied by alkaline volcanism in the whole region [*Tomek and Hall*, 1993]. However, for the latter the density decrease due to thermal expansion, causing the uplift, would have a negative effect on the gravity anomaly. This is not in agreement with the general observation of the low amplitude of the negative gravity anomaly in the foredeep.

Underestimation of the Bouguer gravity field seems to be corrected recently by the re-calibration of the Bouguer gravity anomalies to a new reference normal field and standardization with the western system [*Krolikowski and Petecki*, 1995]. However, the continuous shift of –20 mGals is not sufficient to fit the gravity prediction. Moreover, to the east the modeling gives better results if compared with the "old" gravity data for subloads generating a positive contribution on the gravity field. A possible mechanism causing uplift and generating a positive gravity contribution is an influx of mantle material, which is not isostatically compensated. Indications for such a mechanism are recently predicted by numerical models simulating the rifting in the Pannonian basin [*Huismans et al.*, 1997]. This model gives indications for a transition from passive rifting, dominated by the thermal subsidence and crustal thinning to active rifting, dominated by upward mantle flow to the rifted area causing a general thickening and convecting flow in the mantle. The uncertainty in the absolute gravity field keeps us from drawing further conclusions on the possible mechanism for the overall uplift.

Apart from this passive elevation of the foreland, recent thrust activity is also observed, causing local uplift [*Leichmann and Hejl*, 1996]. In the distal region of the most western part of the foredeep, unpublished seismic lines clearly show recent thrust activity deforming the Karpathian and Badenian layers, suggesting 400–500 m tectonic uplift. Local thrust activity in this area may be triggered by erosion in the foredeep. Since foredeep sediments are easier to erode than basement material of the Bohemian Massif, the passive uplift may first trigger erosion of the foredeep. If we assume after passive uplift an initial erosion of about 120 m sediments, this will generate an isostatic reaction causing 280 m basement uplift under the foredeep, decreasing to zero near the bulge area, leaving a differential uplift of about 130 m at the proximal basin margin. As a result, a sharp topographic contrast may develop between basin and distal foreland. The successive isostatic instability may be compensated by the reactivation of Hercynian thrust fronts in this area. If we further assume possible erosion of the forebulge the basement uplift in this area may be somewhat larger. However, tectonic uplifts of the order of 400-500 m are difficult to explain purely by the indirect effects of passive uplift and erosion. Therefore we should also consider recent tectonic activity in the Bohemian Massif [e.g., *Ilejl et al.*, 1997] to be responsible for uplift in the distal area of the foredeep. Additional analysis

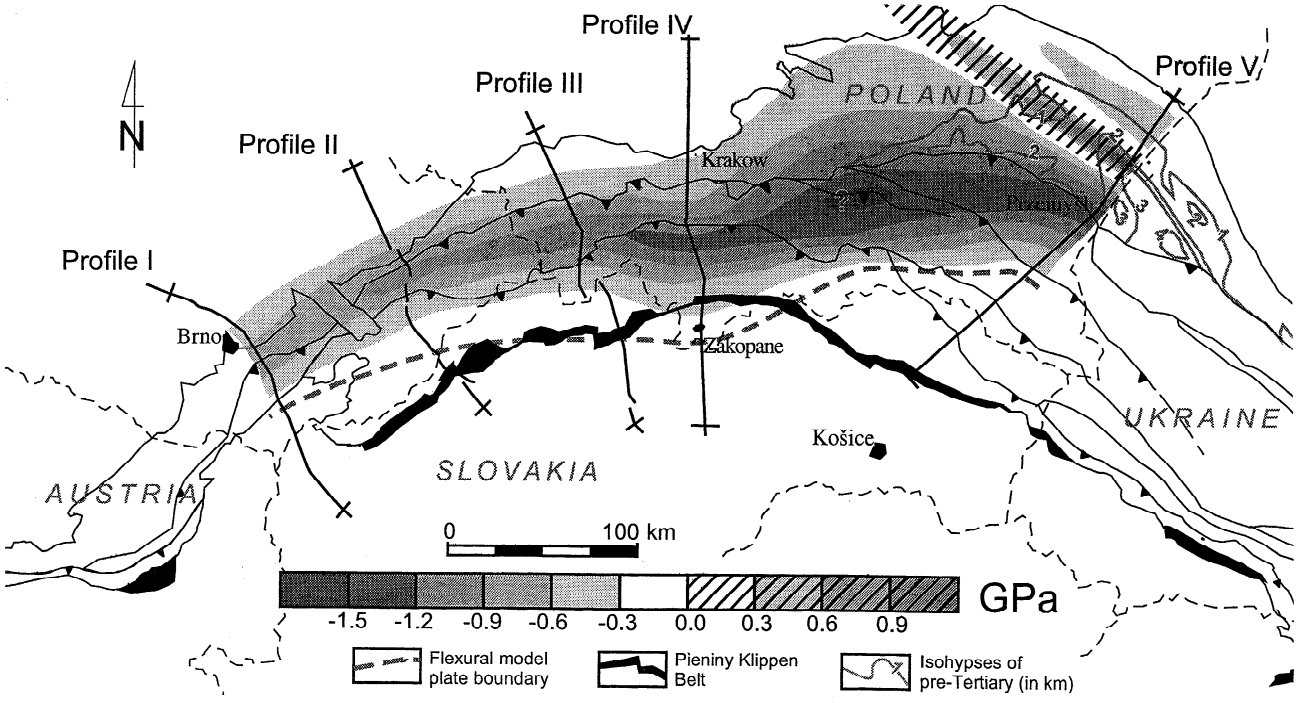

Figure 11. Simplified geological map of the western Carpathians indicating the predicted flexural bending stresses. Areas with predicted bending stresses in excess of ± 1 GPa are characterized by a decrease in EET due to inelastic deformation (brittle faulting at surface and ductile flow at depth).

of the actual stress field and geological field mapping [e.g., *Fodor et al.*, 1999] should be carried out before drawing further conclusions.

8. Coupled or Decoupled Lithosphere?

In lithosphere analyses the terms coupled and decoupled are used in different contexts. In this paper we discuss them in three different ways: in an isostatic sense, in a rheological sense, and in a tectonic sense. Isostatic (de)coupling comes forward in the definition of the effective plate boundary. In the flexural model the down-flexing plate is assumed to carry the surface load of the overthrusting wedge. If this is no longer true, the effective plate boundary is set, which does not mean that the plate does not continue farther under the thrust wedge. Deeper parts of the plate may exert a slab-pull force, which is projected in the model boundary conditions. In other words, a prime requirement for the flexural model is the isostatic coupling between the overlying thrust wedge and the down-flexed plate.

Rheological (de)coupling is discussed earlier [e.g., *McNutt et al.*, 1988; *Burov and Diament*, 1995; *Cloetingh and Burov*, 1996]. It indicates the coupling or decoupling between the rheological layers that build the continental lithosphere. When bending stresses exceed the failure criteria for the upper crust, a decoupling zone may form at that level, and similar processes may occur at Moho level. Figure 9b shows the response of decoupled continental lithosphere to applied stresses. The low EET values that are inferred from the flexural modeling support a scenario in which the European lithosphere under the western Carpathians is completely decoupled in rheological sense.

The tectonic evolution of collisional systems is characterized by two different phases. Different names are proposed in the literature: flysch and molasse phases proposed by *Ricci Luchi* [1986] and accretionary wedge and continental wedge phases proposed by *Sinclair and Allen* [1992]. *Royden* [1993] suggests that the molasse phase is restricted to certain conditions and that some collisional systems never reach the molasse phase. In this respect the western Carpathian system is a typical flysch type of system which only endured soft collision.

Another explanation for the different stages may be the state of lateral coupling or decoupling between the subducting/underthrusting plate and the overthrusting plate [*Ziegler et al.*, 1998]. The flysch stage may be compared with a stage of decoupling between the two colliding plates, typified by the dominant subduction/underthrusting mechanism, and a thrust wedge being built by shallow detached imbrications. In a later stage of collision the plates may become coupled. Deep detachments may develop in the underthrusting plate, involving the upper crust in the thrust belt, producing higher topography and probably changing the facies in the foredeep from flysch to molasse. In this context the western Carpathians are clearly decoupled in a tectonic sense.

9. Conclusions

The tectonic evolution of the Carpathian Arc is characterized by a long complex history of convergence of microplates or stacking of tectonic terrains and closure of the South and North Penninic and Krosno-Tarcau oceans during the Cretaceous to Miocene time span. It is followed by a postcollisional phase during which subcrustal processes including possible phase changes, thermal influence of the adjacent Pannonian basin, and mantle doming or inversion of the intraplate stress field modify the flexural expression in the foredeep. Flexural modeling of the basement deflection of the European lithosphere under the western Carpathians allowed us to resolve some key elements of this complex history. The modeling is constrained by (deep) seismic profiles, numerous wells, and Bouguer gravity anomalies. Furthermore, geological observations as sediment remnants and oblique crustal sutures allowed us to relate the modeling results to tectonic configurations and evaluate new hypotheses.

The deflection in the foredeep is primarily controlled by the subduction/underthrusting process of the European lithosphere under the western Carpathians. It appears likely that small remnants of oceanic slab cause the slab-pull forces, which clearly increase in importance from west to east (V_0 increases from 2.0 10^{11} to 8.0 10^{11} N/m). The subsidence is further enlarged by the positive effect of loading a passive margin (PM) and/or syncollisional phase changes in the crustal root (PC). Both scenarios are able to explain the observation of flat Moho. They produce similar flexural modeling results, and therefore without additional data we cannot constrain their control on the formation of the foredeep.

The assumed density distribution in the flexural model predicts a Bouguer anomaly whose shape is in good agreement with the observed Bouguer anomaly. However, some degrees in freedom remain for the absolute fit to the observations. Differences in the reference models used for the Bouguer anomaly data and uncertainties in the mechanism responsible for the postcollisional uplift prevent us from making better model predictions. Yet the flexural modeling clearly indicates the importance of postcollisional regional uplift, modifying the initial basin width and possibly affecting the gravity field. The amount of uplift is well quantified by the modeling: it is most pronounced in vicinity of the Bohemian Massif, but it is important for the whole region and is supported by the existence of remnants of marine foredeep sediments beyond the distal margin of the basin. Mechanisms responsible for such regional uplift may be related to flow of mantle material away from the rifting Pannonian basin [*Huismans et al.*, 1997]. This process would give a regional positive contribution (~25 mGals) to the Bouguer anomaly, which is in agreement with the general low amplitude of the gravity minimum under the western Outer Carpathians. A thermally induced uplift would give a negative contribution to the Bouguer anomaly of ~25 mGals. Additionally, we must consider that uplift is also controlled by reactivation of thrust fronts, especially in the margins of the Bohemian Massif.

Apart from narrowing the basin because of the regional uplift, the predicted basin configuration is clearly controlled by lateral changes in the strength of the European lithosphere. These changes are not in first order related to differences in the rheological properties of the European lithosphere but are dominated by the amount of internal deformation caused by curvature during the subduction/underthrusting process under the Carpathians. Weakening of the elastic plate, represented by low EET values, coincides well with areas of maximum

flexural bending stress in the lithosphere (Figure 11). The low EET values are in agreement with predictions of *Burov and Diament* [1995], who explain reduction of EET with inelastic deformation (brittle failure and ductile flow).

In the eastern part of the western Carpathians (profile V, Figure 1) the widening of the foredeep reflects the lateral interaction of the western and eastern subduction/underthrusting systems. Although neither the 2–D modeling nor the thin-elastic-plate assumption can quantify the interaction, it is clear that in this region the strong flexural bending could have led to the reactivation of normal faults. This hypothesis is opposite to the general assumption that normal faults in collisional settings become inverted. An important consequence of brittle failure and normal fault reactivation in the foreland is that the subduction/underthrusting system and overthrusting wedge system are tectonically decoupled [*Ziegler et al.*, 1998]. This is in contrast with the Romanian eastern Carpathians where precollisional structures in the foreland are inverted and basement seems to be involved in the overthrusting system [*Ellouz et al.*, 1994; *Matenco et al.*, 1997].

Acknowledgments. We thank Vlasta Dvorakova for assistance in collecting data. Jeremy Hall and the Memorial University of Newfoundland are thanked for the migrated version of the 8HR deep seismic line. We thank M. Fernàndez for the constructive review. Support provided by the EUROPROBE-PANCARDI Project is gratefully acknowledged. R.Z. thanks the Earth and Life Sciences Branch (ALW) of the Netherlands Organization for Scientific Research (NWO) for funding project 751.360.003. This is Netherlands Research School of Sedimentary Geology contribution 981101.

References

Andeweg, A., and S. Cloetingh, Flexure and 'unflexure' of the Northern Alpine German-Austrian Molasse Basin: Constraints from forward tectonic modelling, *Geol. Soc. Spec. Publ., 134*, 403-422, 1998.

Andrusov, D., *Grundriss der Tektonik der Nordlichen Karpaten*, 188 pp., Verlag, Bratislava, Slovakia, 1968.

Austrheim, H., Eclogitization of the deep crust in continent collision zones, *C.R. Acad. Sci., Sér. II, 319*, 761-774, 1994.

Birkenmajer, K., Major strike-slip faults of the Pieniny Klippen Belt and the Tertiary rotation of the Carpathians, *Publ. Inst. Geophys. Pol. Acad. Sci., A-16*, 101-115, 1985.

Bois, C., The evolution of the layered lower crust and the Moho through geological time in Western Europe: Construction of deep seismic reflection profiles, *Terra Nova, 4*, 99-108, 1992.

Bojdys, G., and M. Lemberger, Three-dimensional gravity modelling of Earth's crust and upper mantle in the Polish Carpathians, *Ann. Soc. Geol. Pol., 56*, 3-4, 1986.

Bousquet, R., B. Goffe, P. Henry, X. Le Pichon, and C. Chopin, Kinematic, thermal and petrological model of the Central Alps: Lepontine metamorphism in the upper crust and eclogitisation of the lower crust, *Tectonophysics, 273*, 105-127, 1997.

Burov, E.B., and M. Diament, The effective elastic thickness (T_e) of continental lithosphere: What does it really mean?, *J. Geophys. Res., 100*, 3905-3927, 1995.

Cloetingh, S., and E.B. Burov, Thermomechanical structure of European continental lithosphere: constraints from rheological profiles and EET estimates, *Geophys. J. Int., 124*, 695-723, 1996.

Davies, J.H., and F. Von Blanckenburg, Slab breakoff: A model of lithosphere detachment and its test in the magmatism and deformation of collisional orogens, *Earth Planet. Sci. Lett., 129*, 85-102, 1995.

Desegaulx, P., H. Kooi, and S. Cloetingh, Consequences of foreland basin development on thinned continental lithosphere: Application to the Aquitaine Basin (SW France), *Earth Planet. Sci. Lett., 106*, 116-132, 1991.

Dewey, J.F., and J.M. Bird, Mountain belts and the new global tectonics, *J. Geophys. Res., 75*, 2625-2647, 1970.

Downes, H., and O. Vaselli (Eds.), Neogene and related magmatism in the Carpatho-Pannonian region, *Acta Vulcanol., 7*, 290 pp., 1995.

Ellouz, N., F. Roure, M. Sandulescu, and D. Badescu, Balanced cross sections in the eastern Carpathians (Romania): A tool to quantify Neogene dynamics, in *Geodynamic Evolution of Sedimentary Basins*, edited by F. Roure et al., pp. 305-325, Technip, Paris, 1994.

Fodor, L., L. Csontos, G. Bada, I. Györfi, and L. Benkovics, Tertiary tectonic evolution of the Pannonian basin system and neighbouring orogens: a new synthesis of paleostress data, *Geol. Soc. Spec. Publ., in press*, 1999.

Hejl, E., D. Coyle, N. Lal, P.v.d. Haute, and G.A. Wagner, Fission-track dating of the western border of the Bohemian massif: Thermochronology and tectonic implications, *Geol. Rundsch., 86*, 210-219, 1997.

Horvath, F., Towards a mechanical model for the formation of the Pannonian Basin, *Tectonophysics, 225*, 333-357, 1993.

Horvath, F., and S. Cloetingh, Stress-induced late-stage subsidence anomalies in the Pannonian Basin, *Tectonophysics, 266*, 287-300, 1996.

Huismans, R.S., Y.Y. Podladchikov, and S.A.P.L. Cloetingh, The transition from passive to active rifting: the Pannonian basin, an application. Results from dynamic modelling, *Terra Nova Abstr., 9*, 96, 1997.

Karnkowski, P., Of age of flysch Carpathian overthrust (in Polish), *Nafta, 11*, 293-296, 1986.

Kovac, M., D. Plasienka, and C. Tomek, Cenozoic convergence history of the Bohemian Massif and central Western Carpathians, *Terra Nova Abstr., 4*, 37, 1992.

Krolikowski, C., and Z. Petecki, Gravimetric atlas of Poland, Map, Panstwowy Inst. Geol., Warsaw, 1995.

Lankreijer, A., M. Kovac, S. Cloetingh, P. Pitonak, M. Hloska, and C. Biermann, Quantitative subsidence analysis and forward modelling of the Vienna and Danube basins: Thin-skinned versus thick-skinned extension, *Tectonophysics, 252*, 433-451, 1995.

Lankreijer, A., V. Mocanu, and S. Cloetingh, Lateral variations in lithosphere strength in the Romanian Carpathians: constraints on basin evolution, *Tectonophysics, 272*, 269-290, 1997.

Lankreijer, A.C., M. Bielik, S. Cloetingh, and D. Majcin, Rheology predictions across the Western Carpathians, Bohemian Massif and the Pannonian basin: Implications for tectonic scenarios, *Tectonics, in press*, 1999.

Laubscher, H., Material balance in alpine orogeny, *Geol. Soc. Am. Bull., 100*, 1313-1328, 1988.

Lefeld, J., and J. Jankowski, Model of deep structure of the Polish Inner Carpathians, *Publ .Inst. Geophys. Pol. Acad. Sci., 175*, 71-100, 1985.

Leichmann, J., and E. Hejl, Quaternary tectonics at the eastern border of the Bohemian massif: New outcrop evidence, *Geol. Mag., 133*, 103-105, 1996.

Lillie, R.J., M. Bielik, V. Babuska, and J. Plomerova, Gravity modelling of the lithosphere in the Eastern Alpine-Western Carpathian-Pannonian Basin region, *Tectonophysics, 231*, 215-235, 1994.

Matenco, L., R. Zoetemeijer, S. Cloetingh, and C. Dinu, Tectonic flexural modelling of the Romanian Carpathians foreland system, *Tectonophysics, 282*, 147-166, 1997.

Mayerova, M., J. Nehybka, M. Novotny, P. Sedlak, P. Hunacek, and I. Viscor, *Reinterpretation of Profile K III*, Geophyzika, Brno, Czechoslovakia, 1983.

McNutt, M.K., M. Diament, and M.G. Kogan, Variations of elastic plate thickness at continental thrust belts, *J. Geophys. Res., 93*, 8825-8838, 1988.

Millan, H., B.T. Den, J. Verges, M. Marzo, J.A. Munoz, E. Roca, J. Cires, R. Zoetemeijer, S. Cloetingh, and C. Puigdefabregas, Palaeo-elevation and effective elastic thickness evolution at mountain ranges: Inferences from flexural modelling in the Eastern Pyrenees and Ebro Basin, *Mar. Pet. Geol., 12*, 917-928, 1995.

Mocanu, V.I., and F. Radulescu, Geophysical features of the Romanian Teritory, *Rom. J. Tecton. Reg. Geol., 75*, 17-36, 1994.

Moretti, I., and L. Royden, Deflection, gravity anomalies and tectonics of doubly subducted continental lithosphere: Adriatic and Ionian seas, *Tectonics, 7*, 875-893, 1988.

Okaya, N., S. Cloetingh, and S. Mueller, A lithospheric cross-section through the Swiss Alps, II, Constraints on the mechanical structure of a continent-continent collision zone, *Geophys. J. Int., 127*, 399-414, 1996.

Oszczypko, N., and A. Slaczka, An attempt to palinspastic reconstruction of Neogene basins in the Carpathian foredeep, *Ann. Soc. Geol. Pol., 55*, 55-75, 1985.

Oszczypko, N., and A. Slaczka, The evolution of the Miocene basin in the Polish outer Carpathians and their foreland, *Geol. Carpathica, 40*, 23-86, 1989.

Oszczypko, N., R. Zajac, I. Garlicka, E. Mencik, J. Dvorak, and O. Matejovska, Geological map of the substratum of the Tertiary of the western outer Carpathians and their foreland, Map, Panstwowy Inst. Geol., Warsaw, 1989.

Poprawa, D., and J. Nemcok, Atlas of the western outer Carpathians and their foreland, Panstwowy Inst. Geol., Warsaw, 1989.

Quinlan, G.M., and C. Beaumont, Appalachian thrusting, lithospheric flexure, and the Paleozoic stratigraphy of the eastern interior of North America, *Can. J. Earth Sci., 21*, 973-996, 1984.

Ranalli, G., *Rheology of the Earth*, 413 pp., Chapman and Hall, New York, 1987.

Ricci Luchi, F., The Oligocene to Recent foreland basin of the northern Apennines, in *Foreland Basins*, edited by P.A. Allen and P. Homewood, *Spec. Publ. Int. Assoc. Sedimentol., 8*, 105-140, 1986.

Richardson, S.W., and P.C. England, Metamorphic consequences of crustal eclogite production in overthrust orogenic zones, *Earth Planet. Sci. Lett., 42*, 183-190, 1979.

Roure, F., J. Kusmierek, G. Bessereau, E. Roca, and W. Strzetelski, Initial thickness variations and basement-cover relationships in the Western outer Carpathians (southeastern Poland), in *Geodynamic Evolution of Sedimentary Basins*, edited by F. Roure et al., pp. 255-279, Technip, Paris, 1994.

Royden, L., Flexural behavior of the continental lithosphere in Italy: Constraints imposed by gravity and deflection data, *J. Geophys. Res., 93*, 7747-7766, 1988.

Royden, L.H., The tectonic expression of slab pull at continental convergent boundaries, *Tectonics, 12*, 303-325, 1993.

Sinclair, H.D., and P.A. Allen, Vertical versus horizontal motions in the Alpine orogenic wedge: Stratigraphic response in the foreland basin, *Basin Res., 4*, 215-232, 1992.

Slaczka, A., Remarks on morphology of the substratum of the Polish Carpathians, *Carp. Balkan Geol. Assoc., Proc., 10*, 281-290, 1975.

Steininger, F., R.L. Bernor, and V. Fahlbusch, European Neogene marine/ continental chronologic correlations, in *European Neogene Mammal Chronology*, edited by E.H. Lindsay et al., *NATO ASI Ser. A , 180*, 15-46, 1990.

Stockmal, G.S., C. Beaumont, and R. Boutilier, Geodynamic models of convergent margin tectonics: Transition from rifted margin to overthrust belt and consequences for foreland-basin development, *AAPG Bull., 70*, 181-190, 1986.

Szafian, P., F. Horvath, and S. Cloetingh, Gravity constraints on the crustal structure and slab evolution along a trans-Carpathian transect, *Tectonophysics, 272*, 233-248, 1997.

Tomek, C., Geophysical investigation of the Alpine-Carpathian arc, *Mem. Soc. Geol. Fr., 154*, 167-199, 1988.

Tomek, C., Deep crustal structure beneath the central and inner West Carpathians, *Tectonophysics, 226*, 417-432, 1993.

Tomek, C., and J. Hall, Subducted continental margin imaged in the Carpathians of Czechoslovakia, *Geology, 21*, 535-538, 1993.

Tomek, C., L. Dvorakova, J. Ibrmajer, R. Jiricek, and T. Korab, Crustal profiles of active continental collisional belt: Czecho-Slovak deep seismic reflection profiling in the Western Carpathians, *Geophys. J. R. Astron. Soc., 89*, 383-388, 1987.

Torge, W., *Gravimetry*, 465 pp., Walter De Gruyter, Hawthorne, N. Y., 1989.

Turcotte, D.L., and G. Schubert, *Geodynamics, Applications of Continuum Physics to Geological Problems*, 450 pp., John Wiley New York, 1982.

Uhlig, V., Uber die Tektonik der Karpaten, *Acad. Wiss. Mater. Nat., 116*, 871-982, 1907.

Van Wees, J.D., and S. Cloetingh, A finite-difference technique to incorporate spatial variations in rigidity and planar faults into 3-D models for lithospheric flexure, *Geophys. J. Int., 117*, 179-195, 1994.

Van Wees, J.D., and R.A. Stephenson, Quantitative modelling of basin and rheological evolution of the Iberian Basin (central Spain): Implications for lithospheric dynamics of intraplate extension and inversion, *Tectonophysics, 252*, 163-178, 1995.

Wdowiarz, S., Zagadniene Poludniowo-Wschodniego Przedluzenia aulakogenu Srodkowopolskiego w geosynklinie Karpackiej, *Przeglad Geol., 31*, 15-21, 1983.

Wdowiarz, S., and S. Jucha, North-western extension of the Borislav-Pokutse Zone of deep-seated folds in the Polish Carpathians, *Geol. .Pol., 4*, 7-26, 1981.

Wortel, M.J.R., W. Spakman, and S. Yoshioka, Slab detachment and non-stationary processes in subduction zones: Evidence from the Mediterranean/ Carpathian region (abstract), *Eos Trans. AGU, 74*, (43), 92, 1993.

Ziegler, P.A., J.-D. Van Wees, and S. Cloetingh, Mechanical controls on collision-related compressional intraplate deformation, *Tectonophysics, 300*, 103-129, 1998.

Zoetemeijer, R., P. Desegaulx, S.A.P.L. Cloetingh, F. Roure, and I. Moretti, Lithospheric dynamics and tectonic-stratigraphic evolution of the Ebro Basin, *J. Geoph. Res., 95*, 2701-2711, 1990.

Zytko, K. et al., Geological map of the western outer Carpathians and their foreland without Quaternary formations, Map, Panstwowy Inst. Geol., Warsaw, 1989.

S. Cloetingh and R. Zoetemeijer, Institute of Earth Sciences, Vrije Universiteit, De Boelelaan 1085, 1081 HV Amsterdam, Netherlands.
(cloeting@geo.vu.nl; zoete@geo.vu.nl)

Č. Tomek, Intitut für Geologie und Paläontologie, Universität Salzburg, Hellbrunnerstrasse 34/III, A-5020 Salzburg, Austria.
(Cestmir.Tomek@sbg.ac.at)

(Received February 19, 1998;
revised September 11, 1998;
accepted September 11, 1998.)